# Acidity and catalytic activity of the mesoporous aluminosilicate molecular sieve MCM-41

Robert Mokaya [1], William Jones, Zhaohua Luan, Maria D. Alba and Jacek Klinowski

*Department of Chemistry, University of Cambridge, Lensfield Road, Cambridge CB2 1EW, UK*

The acidity and catalytic properties of aluminosilicate mesoporous molecular sieves with the MCM-41 structure and bulk Si/Al ratios in the 10–60 range have been investigated. The incorporation of 4-coordinate aluminium into the structure of MCM-41 generates both Brønsted and Lewis acid sites in amounts increasing with the degree of incorporation. However, the Brønsted/Lewis acid population ratio is independent of the content of aluminium. The number and strength of acid sites generated are comparable to those of a pillared acid-activated clay and lower than in zeolite H-Y with Si/Al = 3.65. Aluminosilicate MCM-41 is a moderate catalyst for the conversion of cumene which proceeds predominantly via catalytic cracking to propene and benzene. The sample of MCM-41 with the highest content of framework aluminium (Si/Al = 10) has the largest number of Brønsted acid sites and exhibits highest catalytic activity.

**Keywords:** aluminosilicate MCM-41; acidity; catalytic activity; cumene conversion

## 1. Introduction

Over the past decade considerable effort has been devoted to developing mesoporous materials to bridge the gap between microporous solids (such as zeolites) and macroporous solids (amorphous aluminosilicates etc.). Materials with pore diameters in the mesopore range and with a narrow pore size distribution have potential applications in catalysis and as host structures in occlusion chemistry. The "pillaring" method, which gives expanded layered structures, has been extensively investigated [1,2]. Although mesoporosity is observed in some pillared materials, the pore size distribution is broader and less well defined than in zeolites. A major breakthrough has been the synthesis by Mobil researchers of a family of mesoporous molecular sieves, designated M41S, with pore diameters in the 1.5–10 nm range [3]. These materials are prepared using liquid crystal templates, probably via a self-assembly mechanism whereby positively charged quaternary ammonium micelles act as templates for the negatively charged silicate framework precursors. Calcination results in the decomposition of the organic template to yield a mesoporous material with a hexagonally arranged array of uniform pores.

Because of their extensive internal space, mesoporous molecular sieves are potentially useful as heterogeneous catalysts. Catalytic properties of molecular sieves rely on the presence of active (e.g. acidic) sites in their frameworks. In the case of MCM-41, the most extensively studied member of the M41S family, active sites may be generated by the incorporation of heteroatoms into its

electrically neutral purely siliceous framework. Aluminium [4–6], vanadium [7], titanium [8], manganese [9], iron [10] and boron [11] have been isomorphously substituted. The incorporation of Al is particularly important as it gives rise to Brønsted acid sites in the form of "bridging" SiOHAl hydroxyl groups associated with the framework aluminium. Much effort has therefore been devoted to the introduction of 4-coordinate Al into the MCM-41 framework. We have recently prepared MCM-41 materials with Si/Al ratios as low as 2.5 and have shown that the nature of the source of Al is crucial in determining the location and coordination of Al in the material [5]. Here we report our studies of the acidity and catalytic properties of a range of aluminosilicate MCM-41 with bulk Si/Al ratios in the 10–60 range.

In order to evaluate the amount and type of acid sites, we have used the "diagnostic" bases cyclohexylamine and pyridine. Temperature programmed desorption (TPD) of cyclohexylamine and infrared spectroscopy (IR) of adsorbed pyridine can provide important information: the sorptive properties of the bases and their different basicity enable a clear distinction to be made between the Lewis and the Brønsted acid sites and between weak and strong acid sites. Thus cyclohexylamine, the stronger base ($pK_b = 3.3$), interacts with both weak and strong acid sites, while pyridine ($pK_b = 8.8$) interacts only with relatively strong sites. The test reaction was the cracking/dehydrogenation of cumene which is often used to characterise the acidity of solid acid catalysts [12,13]. Our results indicate that the incorporation of aluminium in the MCM-41 framework generates both Brønsted and Lewis acid sites, and that the number of such sites depends on the amount of incorporated aluminium. Aluminosilicate MCM-41 possesses

---

[1] To whom correspondence should be addressed.

considerable catalytic activity in this reaction. For the materials studied, MCM-41 with the highest framework aluminium content ($Si/Al = 10$) has the largest number of acid sites and is the most effective catalyst.

## 2. Experimental

### 2.1. Synthesis

The sources of silicon and aluminium were Cab-O-Sil M-5 fused silica (BDH) and aluminium sulphate (Fluka-Garamtie), respectively. A solution of cetyltrimethylammonium hydroxide was prepared by batch exchange of a 25 wt% aqueous solution of $C_{16}H_{33}(CH_3)_3NCl$ using the IRA-420(OH) ion-exchange resin (both from Aldrich). A 25% aqueous solution of tetramethylammonium hydroxide was obtained from Aldrich.

Aluminosilicate MCM-41 was prepared using Cab-O-Sil M-5 fused silica as the source of silicon. A typical synthesis procedure was as follows. (1) 10 g of solution of tetramethylammonium hydroxide (TMAOH) was combined with 5.9 g sodium silicate dispersed in 50 g water with stirring, and 34.2 g of $C_{16}H_{33}(CH_3)_3NCl/$ OH (CTACl/OH) solution and 4.52 g silica was added and stirred for 2 h. (2) A required amount of the desired aluminium sulphate was dissolved in water and then slowly added to the gel. (3) The pH was adjusted with dilute sulphuric acid to 11.5, and the mixture was transferred into a teflon-lined autoclave and heated to 150°C for 48 h. The molar composition of the final gel mixtures was $SiO_2 : 0.27CTACl/OH : 0.13Na_2O : 0.26TMAOH : 60H_2O : (0-0.5)Al_2O_3$. (4) The solid product was centrifuged, filtered, washed with distilled water, dried in air at 100°C and finally calcined at 550°C for 24 h. The samples are designated as MCM-41-$X$, where $X = 10$, 20, 40 and 60 are the Si/Al ratios in the synthesis gel. $NH_4^+$-MCM-41 was obtained by repeated ion exchange of $Na^+$-MCM-41 with 1 M aqueous solution of $NH_4Cl$. Calcination of $NH_4^+$-MCM-41 at 550°C for 12 h gave $H^+$-MCM-41.

### 2.2. Sample characterization

*Composition.* Elemental composition was determined by X-ray fluorescence (XRF). Table 1 shows that the molar Si/Al ratios of the parent $Na^+$-MCM-41-$n$ samples are in close agreement with the composition of gel mixtures, indicating that Al and Si in the gel are incorporated into the solid in equal proportions. The molar Si/Al ratios of the $H^+$-MCM-41-$n$ samples calculated from the $^{27}Al$ NMR spectra are also given.

*X-ray diffraction.* XRD patterns were recorded using a Philips 1710 powder diffractometer with Cu K$\alpha$ radiation (40 kV, 40 mA), 0.025° step size and 1 s step time.

*Solid-state NMR.* $^{27}Al$ magic-angle-spinning (MAS)

Table 1
Elemental composition of the gel mixture and samples of aluminosilicate MCM-41

|              | Si/Al ratio |      |      |      |
| ------------ | ----------- | ---- | ---- | ---- |
| gel mixture  | 10          | 20   | 40   | 60   |
| products (by XRF) | 10.4   | 21.5 | 43.0 | 71.0 |

NMR spectra were recorded at 9.4 T using a Chemagnetics CMX-400 spectrometer with zirconia rotors 4 mm in diameter spun at 8 kHz. The spectra were measured at 104.3 MHz with 0.3 s recycle delays and corrected by subtracting the spectrum of the empty MAS rotor. Short $\pi/20$ radiofrequency pulses were used to ensure that they are quantitatively reliable [14]. External $Al(H_2O)_6^{3+}$ was used as a reference. All samples were fully hydrated prior to the measurements [15].

### 2.3. Acidity measurements

The Brønsted acidity was measured using thermogravimetric analysis (TGA) following adsorption of cyclohexylamine on the samples [16]. This method determines the number of protons capable of interacting with the base. The weight loss between 240 and 420°C is used to quantify the acidity in mmol of cyclohexylamine desorbed. A relatively high lower temperature limit (240°C) was chosen so that differences in the amount of the physisorbed base do not affect the results. FTIR spectra of chemisorbed pyridine were measured using a Nicolet 205 FTIR spectrometer. 25–30 mg of each sample was pressed (for 2 min at 10 ton/$cm^2$ pressure under vacuum) into a self-supporting wafer 13 mm in diameter. The wafers were calcined under vacuum ($10^{-3}$ Torr) at 500°C for 2 h followed by exposure to pyridine vapour at ambient temperature and heating at 100°C for 1 h to allow the pyridine to permeate the sample. The wafers were then allowed to cool to ambient temperature and evacuated for 1 h, following which 1 h thermal treatments in the 100–500°C temperature range were performed and the spectra recorded at ambient temperature.

### 2.4. Catalytic testing

The cracking/dehydrogenation of cumene was performed using a pulse microreactor with a helium flow of 25 ml/min. The catalyst bed (0.05 g; 30–60 mesh) was first activated for 1.5 h at 500°C under helium (25 ml/min). During the measurements the volume of a cumene pulse was 0.25 μl (1.8 μmol). Several initial pulses were given in order to saturate the catalyst and stabilise the conversion prior to the catalytic runs. The reaction products were separated and analysed using a Carlo Erba HRGC 5300 gas chromatograph on line with the microreactor.

# 3. Results and discussion

## 3.1. Sample characterisation

Powder XRD patterns of the calcined as-synthesised ($Na^+$-MCM-41) and protonated ($H^+$-MCM-41) samples with Si/Al molar ratios from 10 to 60 given in fig. 1 are typical of MCM-41 materials as described by Beck et al. [3]. All aluminosilicate samples give lower quality XRD patterns than the purely siliceous MCM-41, and the intensity of the (100) peak decreases even at very low levels of aluminium incorporation. The (110) and (200) peaks are ill-defined and overlap to give a single broad line. It is therefore clear that the structure of aluminosilicate MCM-41 is less uniform than that of purely siliceous MCM-41. Furthermore, patterns from $H^+$-MCM-41 samples (which contain extra-framework Al) are weaker and broader than those of the corresponding parent $Na^+$-MCM-41, indicating that the formation of non-structural Al is accompanied by the collapse of portions of the aluminosilicate framework.

Earlier work has shown that the $^{27}Al$ MAS NMR spectra of the parent $Na^+$-MCM-41 gives a single sharp resonance from 4-coordinate Al at 53.0 ppm indicating that when aluminium sulphate is used as the source of Al, aluminium from the synthesis gel is incorporated exclusively into the framework [5]. Upon calcination to remove the template, the sharp $^{27}Al$ peak broadens, but

its absolute intensity does not decrease [5]. The $^{27}Al$ MAS NMR spectra of samples $H^+$-MCM-41-$n$ shown in fig. 2 indicate that in the course of ammonium exchange and calcination at 550°C some aluminium is removed from the MCM-41 framework. However, the intensity of the line at ca. 53 ppm is fully consistent with the Si/Al ratio of the parent $Na^+$-MCM-41: the same proportion of framework aluminium is removed during the heat treatment.

## 3.2. Acidity of aluminosilicate MCM-41

### 3.2.1. Brønsted acidity.

Column 3 in table 2 gives the concentrations of Brønsted acid sites determined using cyclohexylamine as the probe molecule. The method measures the population of those sites which are accessible and sufficiently strong to interact with the base. In calculating the acidity values it was assumed that each molecule interacts with one Brønsted acid site [16]. As indicated earlier, the acidity values are expressed per weight of sample at 240°C so as to exclude any differences in the amount of physisorbed base. As expected, the purely siliceous MCM-41 undergoes no discernable weight loss between 240 and 420°C, indicating that there are no acid sites capable of interacting with the base. The very small number of acid sites detected in the equivalent $H^+$ form ($H^+$-MCM-41) are most likely due to weakly acidic silanol groups to
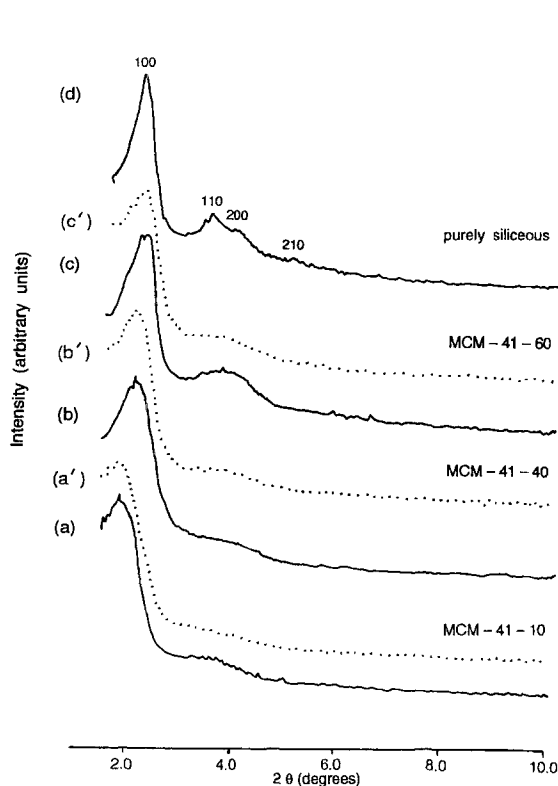


Fig. 1. Solid lines: XRD patterns of (a)$Na^+$-MCM-41-10; (b) -40; (c) -60, and (d) purely siliceous MCM-41. Dotted lines: patterns of (a′) $H^+$-MCM-41-10; (b′) -40; (c′) -60.
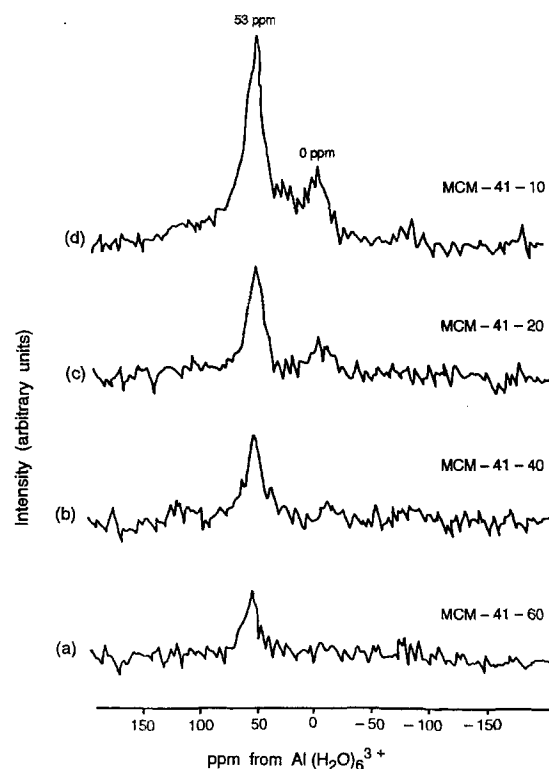


Fig. 2. $^{27}Al$ MAS NMR spectra on the absolute intensity scale of $H^+$-MCM-41 prepared from $Na^+$-MCM-41 and calcination at 550°C for 24 h. (a) $H^+$-MCM-41-60; (b) -40; (c) -20; (d) -10. All samples were hydrated and equilibrated with room air prior to experiments.

Table 2
Acidity of aluminosilicate MCM-41 with different contents of structural aluminium determined using temperature-programmed desorption (TPD) of cyclohexylamine

| Sample | Na$^+$-form (mmol CHA$^a$/g at 240°C) | H$^+$-form (mmol H$^+$/g at 240°C) |
|---|---|---|
| MCM-41 | – | 0.05 |
| MCM-41-60 | 0.32 | 0.41 |
| MCM-41-40 | 0.36 | 0.48 |
| MCM-41-20 | 0.40 | 0.54 |
| MCM-41-20 | 0.52 | 0.66 |
| zeolite H-Y | – | 1.49 |
| PILC$^b$ | | 0.43 |
| PAAC$^c$ | | 0.66 |

$^a$ CHA = cyclohexylamine.
$^b$ PILC = pillared (intercalated layered) clay [12].
$^c$ PAAC = pillared acid-activated clay [12].

which the strongly basic cyclohexylamine is hydrogen-bonded (see fig. 3).

It is clear from the acidity values in table 2 (column 3) that the substitution of aluminium for silicon in the MCM-41 framework generates acid sites which are able to interact with the base. Furthermore, the number of acid sites generated increases as the amount of aluminium in the MCM-41 framework increases. The acidity of the protonated materials is generally higher than that of pillared clays and (in the case of sample H$^+$-MCM-41-10) comparable to that of pillared acid-activated clays [12], but much lower than that of zeolite H-Y (see table 2). The amount of base desorbed from the Na$^+$-form of aluminosilicate MCM-41 (table 2, column 2) is interesting and suggests that during the adsorption process the base may take up sites occupied
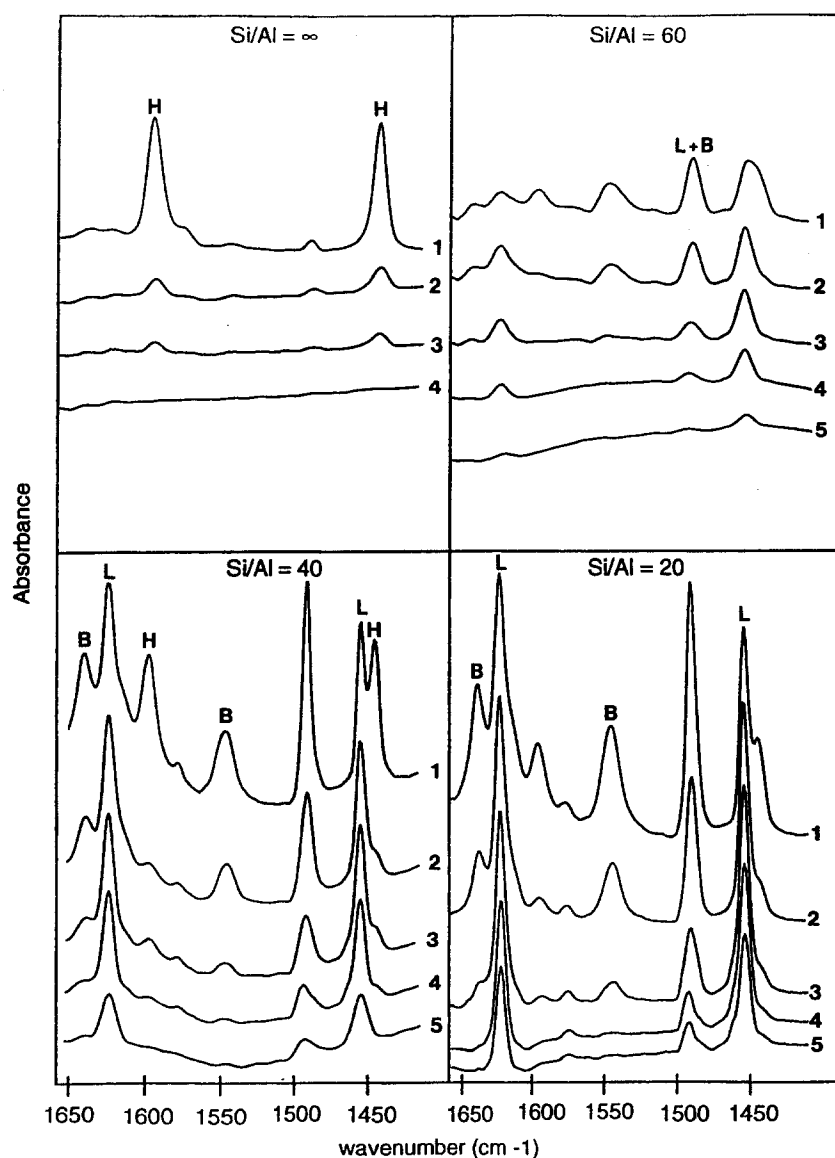


Fig. 3. IR spectra of pyridine adsorbed on H$^+$-MCM-41 samples with various bulk Si/Al ratios following thermal treatment at: (1) 100°C; (2) 200°C; (3) 300°C; (4) 400°C; (5) 500°C. H denotes hydrogen-bonded pyridine: B Brønsted-bound pyridine; L Lewis-bound pyridine.
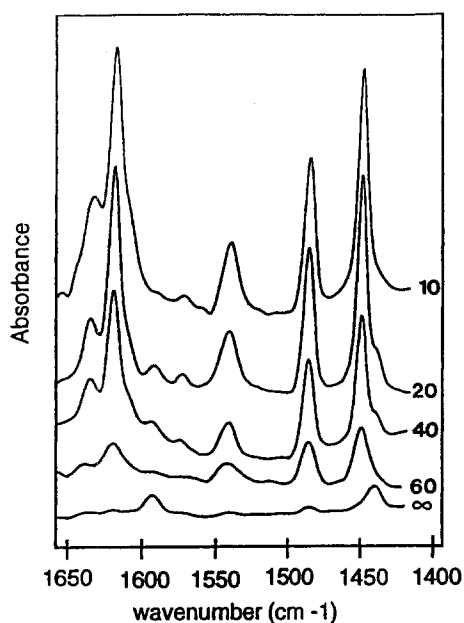
Fig. 4. IR spectra of pyridine adsorbed on H⁺-MCM-41 samples with various bulk Si/Al ratios following thermal treatment at 200°C. Peak assignments as in fig. 3.

by Na⁺ ions by ion exchange. The fact that not all exchangeable Na⁺ sites are occupied by the base explains the difference between the corresponding values in columns 2 and 3. It appears that in all cases the ion-exchange process results in the replacement of 75–80% of the Na⁺ ions with the base, corresponding to an ion-exchange equilibrium. The values of cyclohexylamine desorption for the Na⁺-MCM-41 materials may therefore be regarded as an indication of the number of *poten-*

*tial* H⁺ sites obtainable in the calcined ammonium-exchanged aluminosilicate MCM-41 material. An alternative explanation is that the values in table 2 (column 3) are a measure of the cylohexylamine adsorbed on Lewis acid sites. Indeed, Breen [16b] has shown that for predominantly Lewis acid materials, Lewis-bound cyclohexylamine is desorbed within the temperature range used to calculate the acidity values.

### 3.2.2. Brønsted and Lewis acidity.

Figs. 3, 4, 5 and 7 show the infrared spectra of pyridine in the region 1650–1400 cm⁻¹ following its adsorption on various MCM-41-*n* samples and subsequent thermal treatment at 100–500°C. The samples were calcined in vacuo at 500°C for 2 h prior to exposure to pyridine. All the samples give the expected bands due to hydrogen-bonded pyridine (1447 and 1599 cm⁻¹), Lewis-bound pyridine (1450, 1575 and 1623 cm⁻¹), pyridine bound on Brønsted acid sites (1545 and 1640 cm⁻¹) and a band at 1490 cm⁻¹ attributed to pyridine associated with both Lewis and Brønsted acid sites [17]. The purely siliceous material (fig. 3) contains mainly hydrogen-bonded pyridine most of which is lost after evacuation at 200°C. This observation is consistent with reports on the acidity of pure silica [17,18]. After evacuation at 100°C, all the aluminosilicate materials (see fig. 3) also give spectral bands indicative of hydrogen-bonded pyridine. As with the purely siliceous MCM-41, these bands are lost after evacuation at 200°C. It is interesting to note that as the amount of framework aluminium increases the relative intensity of the hydrogen-bonded pyridine band decreases when compared to the other diagnostic bands.
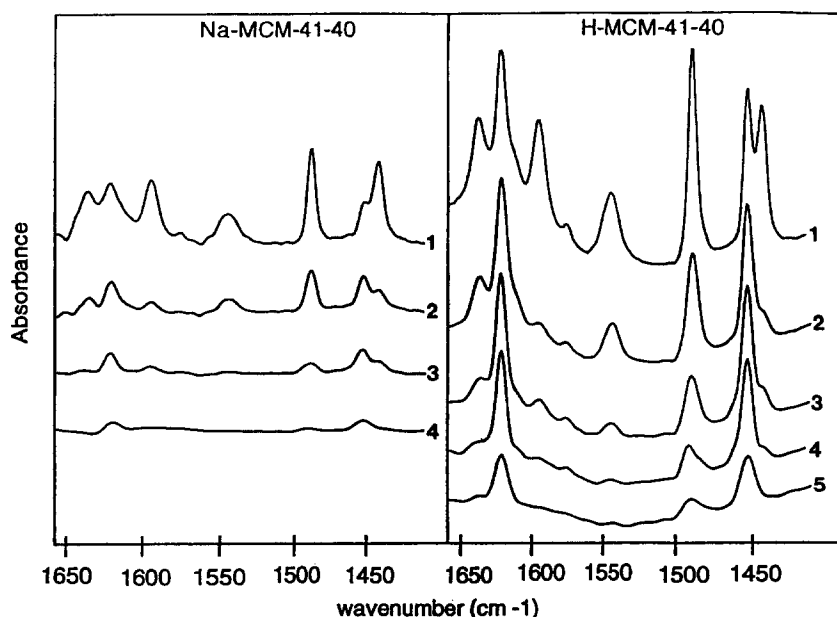


Fig. 5. IR spectra of pyridine adsorbed on samples Na⁺-MCM-41-40 and H⁺-MCM-41-40. Thermal treatment and peak assignments are as in fig. 3.

Infrared spectra of aluminosilicate MCM-41 reveal the presence of both Lewis and Brønsted acid sites. Furthermore, fig. 3 indicates that both Brønsted and Lewis acidity increase as the amount of aluminium in the MCM-41 framework increases, thus showing a clear relationship between framework aluminium and the number of acid sites. This observation is consistent with the results from the sorption of cyclohexylamine (table 2). The relationship between the amount of framework Al and acidity is much clearer in fig. 4 which shows the spectra of all the samples after evacuation at 200°C. The Brønsted/Lewis (B/L) acid ratio calculated from the band areas (for all the aluminosilicate samples) was 0.5. The observed B/L ratio is similar to that previously reported for aluminium containing MCM-41 [6,19]. We further found that the B/L ratio did not change with the bulk Si/Al ratio of the samples. We believe that this is an indication that the proportion of framework aluminium removed during various pretreatments (such as calcination of the $NH_4^+$ exchanged MCM-41 to obtain the protonated materials) did not change with the total amount of framework Al. If the proportion of extra-framework were to increase with the Si/Al ratio, we would expect to see a decrease in the B/L ratio as the Si/Al ratio increases. These arguments are in agreement with our interpretation of the $^{27}Al$ NMR spectra (see fig. 2).

The IR spectra of pyridine adsorbed on $Na^+$- and $H^+$-MCM-41-40 shown in fig. 5 indicate that the acidity of the $H^+$ form is much higher than of the $Na^+$ form. Given the presence of $H^+$ as the charge-balancing cation, the increase in Brønsted acidity is expected. The increased Lewis acidity is clearly related to the presence of extra-framework Al formed during calcination, although, as in the case of zeolites, the precise nature of the Lewis sites is unknown.

All IR spectra indicate that increasing evacuation temperatures reduces the number of acid sites capable of interacting with pyridine. The rate of reduction of the intensity of the bands at 1455 and 1623 $cm^{-1}$ is similar as is the case for the bands at 1540 and 1640 $cm^{-1}$, showing that these bands represent similar species: Lewis- and Brønsted-bound pyridine, respectively. The reduction in the number of Brønsted acid sites appears greater than that of the Lewis sites. This is clearly shown in fig. 6, which shows that the B/L ratio decreases as the evacuation temperature is raised. We have compared the most acidic sample ($H^+$-MCM-40-10) with zeolite $H^+$-Y with Si/Al = 3.65 (fig. 7). Along with fig. 6 the pyridine spectra show that zeolite $H^+$-Y has higher Brønsted acidity.

### 3.3. Catalysis

Table 3 summarizes the results of cumene conversion over the purely siliceous MCM-41 and the aluminosilicate materials with Si/Al ratio of 10, 20, 40 and 60. Zeolite H-Y, pillared clay and pillared acid-activated clay are included for comparison. As expected, neither the $Na^+$- nor the $H^+$-form of the purely siliceous material displays catalytic activity under the conditions of the experiments. On the other hand, aluminosilicate MCM-41-$n$ samples show considerable activity, with the conversion of cumene increasing with the increasing content of framework aluminium. The conversion gives almost exclusively benzene and propene, the cracking products. Only very small amounts of α-methylstyrene, the dehydrogenation product over Lewis acid sites, are found, indicating that the active sites are the Brønsted acid sites. These results are consistent with earlier studies of the conversion of cumene over silica–aluminas [13]. The suggestion that Brønsted acid sites are the active sites is
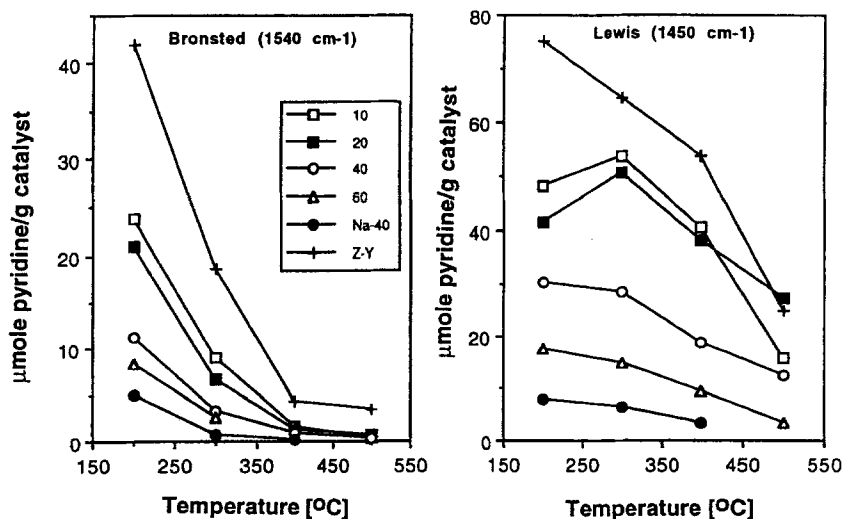


Fig. 6. Acidity of MCM-41 samples with various bulk Si/Al ratios as a function of the temperature of thermal treatment. Acidity of zeolite H-Y is given for comparison. Acidity values were calculated using the extinction coefficients of Hughes and White [18].
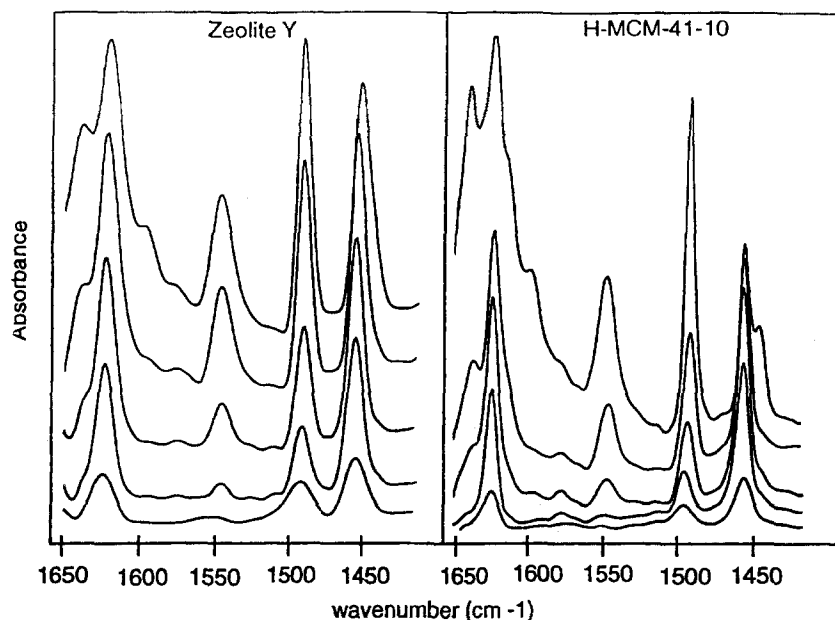
Fig. 7. IR spectra of pyridine adsorbed on H⁺-MCM-41-10 and zeolite H-Y following thermal treatment (top to bottom) 100, 200, 300, 400 and 500°C. Peak assignments are as in fig. 3.

supported by the fact that the lower Brønsted-acidic Na⁺ forms of the materials are less catalytically active than the corresponding H⁺ forms. We note that despite the low activity, Na⁺-MCM-41-$n$ samples exhibit the same product selectivity as their H⁺ counterparts. Furthermore, zeolite H⁺-Y which has higher Brønsted acidity and a higher B/L ratio, especially at high temperatures, shows much higher activity and similar product selectivity. This is a further indication that the active centres are the Brønsted acid sites and that the Brønsted acid sites in zeolite H⁺-Y are stronger than those on aluminosilicate MCM-41. The catalytic activity of the H⁺-MCM-41-$n$ materials is comparable to that of the pillared clay and pillared acid-activated clay. This observation is in agreement with the acidity data in table 2.

## 4. Conclusions

Incorporation of 4-coordinate aluminium into the framework of MCM-41 generates both Brønsted and Lewis acid sites in populations increasing with the amount of framework aluminium. The number and strength of acid sites are both comparable to those on a pillared acid-activated clay but lower than for zeolite H⁺-Y. The Brønsted/Lewis acid ratio is independent of the bulk Si/Al ratio. However, the IR spectra of adsorbed pyridine show that the B/L ratio is very sensitive to temperature. The aluminosilicate MCM-41 materials are moderate catalysts for the conversion of cumene which proceeds predominantly via cracking to propene and benzene. We conclude that aluminosilicate MCM-41-$n$ materials are mildly acidic cracking cat-

Table 3
Cumene hydrocracking over aluminosilicate MCM-41 catalysts

| Sample | % conversion | | | | |
|---|---|---|---|---|---|
| | H⁺-form | | | Na⁺-form | |
| | 300°C | 400°C | 500°C | 400°C | 500°C |
| MCM-41 | | | no catalytic activity | | |
| MCM-41-60 | 8.5 | 33.2 | 48.0 | – | – |
| MCM-41-40 | 10.2 | 35.8 | 49.5 | 2.1 | 6.0 |
| MCM-41-20 | 13.5 | 37.0 | 52.0 | – | – |
| MCM-41-10 | 18.0 | 39.5 | 59.4 | 8.2 | 16.5 |
| zeolite H-Y | 62.5 | 84.0 | 90.8 | – | – |
| PILC[a] | 3.2 | 33.0 | 59.4 | | |
| PAAC[a] | 13.3 | 46.2 | 61.3 | | |

[a] Catalytic data from ref. [12].

alysts, but may accommodate larger substrate molecules than any other molecular sieve.

## Acknowledgement

## References

[1] I.V. Mitchell, ed., *Pillared Layered Structures* (Elsevier, Amsterdam, 1990).

[2] C. Sequeira and M. Hudson, eds., *Multifunctional Mesoporous Inorganic Solids*, NATO ASI Series, Vol. 400 (Kluwer, Amsterdam, 1993).

[3] C.T. Kresge, M.E. Leonowicz, W.J. Roth, J.C. Vartuli and J.S. Beck, Nature 359 (1992) 710;
J.S. Beck, M.C. Vartuli, W.J. Roth, M.E. Leonowicz, C.T. Kresge, K.O. Schmitt, C.T.-W. Chu, D.H. Olson, E.W. Sheppard, S.B. McCullen, J.B. Higgins and J.L. Schlenker, J. Am. Chem. Soc. 114 (1992) 10834.

[4] R. Schmidt, D. Akporiaye, M. Stocker and O.H. Ellestad, J. Chem. Soc. Chem. Commun. (1994) 1493.

[5] Z.H. Luan, C.F. Cheng, W.Z. Zhou and J. Klinowski, J. Phys. Chem. 99 (1995) 1018.

[6] R.B. Borade and A. Clearfield, Catal. Lett. 32 (1995) 267.

[7] K.M. Reddy, I. Moudrakouski and A. Sayari, J. Chem. Soc. Chem. Commun. (1994) 1059.

[8] P.T. Tanev, M. Chibwe and T.J. Pinnavaia, Nature 368 (1994) 321;
A. Corma, M.T. Navarro, J. Pérez-Pariente, J. Chem. Soc. Chem. Commun. (1994) 148.

[9] D. Zhao and D. Goldfarb, J. Chem. Soc. Chem. Commun. (1995) 875.

[10] Z.Y. Yuan, S.Q. Liu, T.H. Chen, Z.J.Z. Wang and H.X. Li, J. Chem. Soc. Chem. Commun. 9 (1995) 973.

[11] A. Sayari, C. Danumah and I.L. Moudrakovski, Chem. Mater. 7 (1995) 813.

[12] R. Mokaya and W. Jones, J. Catal. 153 (1995) 76.

[13] J.W. Ward, J. Catal. 9 (1967) 225; 11 (1968) 251, 259.

[14] P.P. Man, J. Klinowski, A. Trokiner, H. Zanni and P. Papon, Chem. Phys. Lett. 151 (1988) 143.

[15] G.J. Ray, B.L. Meyers and C.L. Marshall, Zeolites 7 (1987) 307.

[16] (a) J.A. Ballantine, J.H. Purnell and J.M. Thomas, Clay Minerals 18 (1983) 347;
(b) C. Breen, Clay Minerals 26 (1991) 487.

[17] E.R. Parry, J. Catal. 2 (1963) 371.

[18] T.R. Hughes and H.M. White, J. Phys. Chem. 71 (1967) 2192.

[19] A. Corma, V. Fornés, M.T. Navarro and J. Pérez-Pariente, J. Catal. 148 (1994) 569.